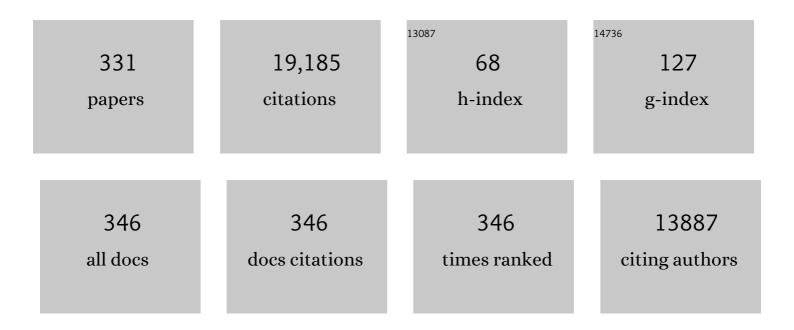
List of Publications by Year in descending order

Source: https://exaly.com/author-pdf/3810769/publications.pdf Version: 2024-02-01



#	Article	IF	CITATIONS
1	Effect of low-energy ion assistance on the properties of sputtered ZrB2 films. Vacuum, 2022, 195, 110688.	1.6	3
2	Oxidation resistance and mechanical properties of sputter-deposited Ti0.9Al0.1B2-y thin films. Surface and Coatings Technology, 2022, 442, 128187.	2.2	7
3	Dense, single-phase, hard, and stress-free Ti0.32Al0.63W0.05N films grown by magnetron sputtering with dramatically reduced energy consumption. Scientific Reports, 2022, 12, 2166.	1.6	8
4	Improving oxidation and wear resistance of TiB2 films by nano-multilayering with Cr. Surface and Coatings Technology, 2022, 436, 128337.	2.2	4
5	Microstructure, mechanical, and corrosion properties of Zr1-xCrxBy diboride alloy thin films grown by hybrid high power impulse/DC magnetron co-sputtering. Applied Surface Science, 2022, 591, 153164.	3.1	3
6	On the nature of planar defects in transition metal diboride line compounds. Materialia, 2022, 24, 101478.	1.3	4
7	Reprint of: Improving oxidation and wear resistance of TiB2 films by nano-multilayering with Cr. Surface and Coatings Technology, 2022, 442, 128602.	2.2	2
8	Oxidation kinetics of overstoichiometric TiB2 thin films grown by DC magnetron sputtering. Corrosion Science, 2022, 206, 110493.	3.0	17
9	Age hardening in superhard ZrB2-rich Zr1-xTaxBy thin films. Scripta Materialia, 2021, 191, 120-125.	2.6	28
10	Where is the unpaired transition metal in substoichiometric diboride line compounds?. Acta Materialia, 2021, 204, 116510.	3.8	21
11	Multifunctional ZrB2-rich Zr1-xCrxBy thin films with enhanced mechanical, oxidation, and corrosion properties. Vacuum, 2021, 185, 109990.	1.6	21
12	X-ray photoelectron spectroscopy analysis of TiBx (1.3 â‰ ê €‰x â‰ ê €‰3.0) thin films. Journal of Va and Technology A: Vacuum, Surfaces and Films, 2021, 39, .	cuumScie	ence
13	Dense Ti0.67Hf0.33B1.7 thin films grown by hybrid HfB2-HiPIMS/TiB2-DCMS co-sputtering without external heating. Vacuum, 2021, 186, 110057.	1.6	9
14	Toward energy-efficient physical vapor deposition: Routes for replacing substrate heating during magnetron sputter deposition by employing metal ion irradiation. Surface and Coatings Technology, 2021, 415, 127120.	2.2	23
15	Synthesis and characterization of CrB2 thin films grown by DC magnetron sputtering. Scripta Materialia, 2021, 200, 113915.	2.6	12
16	Improved oxidation properties from a reduced B content in sputter-deposited TiBx thin films. Surface and Coatings Technology, 2021, 420, 127353.	2.2	24
17	Towards energy-efficient physical vapor deposition: Mapping out the effects of W+ energy and concentration on the densification of TiAlWN thin films grown with no external heating. Surface and Coatings Technology, 2021, 424, 127639.	2.2	15
18	Systematic compositional analysis of sputter-deposited boron-containing thin films. Journal of Vacuum Science and Technology A: Vacuum, Surfaces and Films, 2021, 39, .	0.9	26

#	Article	IF	CITATIONS
19	Thermally induced structural evolution and age-hardening of polycrystalline V1–xMoxN (xÂâ‰^Â0.4) thin films. Surface and Coatings Technology, 2021, 405, 126723.	2.2	11
20	Cubic-structure Al-rich TiAlSiN thin films grown by hybrid high-power impulse magnetron co-sputtering with synchronized Al+ irradiation. Surface and Coatings Technology, 2020, 385, 125364.	2.2	10
21	Improving the high-temperature oxidation resistance of TiB2 thin films by alloying with Al. Acta Materialia, 2020, 196, 677-689.	3.8	65
22	Self-organized columnar Zr0.7Ta0.3B1.5 core/shell-nanostructure thin films. Surface and Coatings Technology, 2020, 401, 126237.	2.2	15
23	Microstructure and materials properties of understoichiometric TiBx thin films grown by HiPIMS. Surface and Coatings Technology, 2020, 404, 126537.	2.2	33
24	Growth of dense, hard yet low-stress Ti0.40Al0.27W0.33N nanocomposite films with rotating substrate and no external substrate heating. Journal of Vacuum Science and Technology A: Vacuum, Surfaces and Films, 2020, 38, .	0.9	13
25	The influence of pressure and magnetic field on the deposition of epitaxial TiBx thin films from DC magnetron sputtering. Vacuum, 2020, 177, 109355.	1.6	14
26	3D-to-2D Morphology Manipulation of Sputter-Deposited Nanoscale Silver Films on Weakly Interacting Substrates via Selective Nitrogen Deployment for Multifunctional Metal Contacts. ACS Applied Nano Materials, 2020, 3, 4728-4738.	2.4	38
27	Adaptive hard and tough mechanical response in single-crystal B1 VNx ceramics via control of anion vacancies. Acta Materialia, 2020, 192, 78-88.	3.8	46
28	Preface for the Festschrift Honoring Dr. Steve Rossnagel. Journal of Vacuum Science and Technology A: Vacuum, Surfaces and Films, 2020, 38, .	0.9	0
29	A review of the intrinsic ductility and toughness of hard transition-metal nitride alloy thin films. Thin Solid Films, 2019, 688, 137479.	0.8	71
30	Paradigm shift in thin-film growth by magnetron sputtering: From gas-ion to metal-ion irradiation of the growing film. Journal of Vacuum Science and Technology A: Vacuum, Surfaces and Films, 2019, 37, .	0.9	94
31	Mechanical properties of VMoNO as a function of oxygen concentration: Toward development of hard and tough refractory oxynitrides. Journal of Vacuum Science and Technology A: Vacuum, Surfaces and Films, 2019, 37, .	0.9	1
32	High-power impulse magnetron sputter deposition of TiBx thin films: Effects of pressure and growth temperature. Vacuum, 2019, 169, 108884.	1.6	21
33	Preface of the special issue "Thin Films Advances―dedicated to the 75th birthday of Professor Joe Greene. Thin Solid Films, 2019, 688, 137494.	0.8	0
34	TiN film growth on misoriented TiN grains with simultaneous low-energy bombardment: Restructuring leading to epitaxy. Thin Solid Films, 2019, 688, 137380.	0.8	7
35	Strategy for simultaneously increasing both hardness and toughness in ZrB2-rich Zr1â^'xTaxBy thin films. Journal of Vacuum Science and Technology A: Vacuum, Surfaces and Films, 2019, 37, .	0.9	42
36	Corrosion Resistant TiTaN and TiTaAlN Thin Films Grown by Hybrid HiPIMS/DCMS Using Synchronized Pulsed Substrate Bias with No External Substrate Heating. Coatings, 2019, 9, 841.	1.2	5

#	Article	IF	CITATIONS
37	Time evolution of ion fluxes incident at the substrate plane during reactive high-power impulse magnetron sputtering of groups IVb and VIb transition metals in Ar/N2. Journal of Vacuum Science and Technology A: Vacuum, Surfaces and Films, 2018, 36, .	0.9	31
38	Effects of surface vibrations on interlayer mass transport: <i>Ab initio</i> molecular dynamics investigation of Ti adatom descent pathways and rates from TiN/TiN(001) islands. Physical Review B, 2018, 97, .	1.1	21
39	Controlling the B/Ti ratio of TiBx thin films grown by high-power impulse magnetron sputtering. Journal of Vacuum Science and Technology A: Vacuum, Surfaces and Films, 2018, 36, .	0.9	46
40	Enhanced Ti0.84Ta0.16N diffusion barriers, grown by a hybrid sputtering technique with no substrate heating, between Si(001) wafers and Cu overlayers. Scientific Reports, 2018, 8, 5360.	1.6	25
41	Elastic properties and plastic deformation of TiC- and VC-based pseudobinary alloys. Acta Materialia, 2018, 144, 376-385.	3.8	45
42	Low temperature (<i>T</i> s/ <i>T</i> m < 0.1) epitaxial growth of HfN/MgO(001) via reactive HiPII with metal-ion synchronized substrate bias. Journal of Vacuum Science and Technology A: Vacuum, Surfaces and Films, 2018, 36, .	MS 0.9	23
43	Self-structuring in Zr1â^'xAlxN films as a function of composition and growth temperature. Scientific Reports, 2018, 8, 16327.	1.6	9
44	Growth and mechanical properties of 111-oriented V0.5Mo0.5Nx/Al2O3(0001) thin films. Journal of Vacuum Science and Technology A: Vacuum, Surfaces and Films, 2018, 36, .	0.9	15
45	Recent developments in surface science and engineering, thin films, nanoscience, biomaterials, plasma science, and vacuum technology. Thin Solid Films, 2018, 660, 120-160.	0.8	27
46	V0.5Mo0.5Nx/MgO(001): Composition, nanostructure, and mechanical properties as a function of film growth temperature. Acta Materialia, 2017, 126, 194-201.	3.8	23
47	Effects of incident N atom kinetic energy on TiN/TiN(001) film growth dynamics: A molecular dynamics investigation. Journal of Applied Physics, 2017, 121, .	1.1	31
48	Controlling the boron-to-titanium ratio in magnetron-sputter-deposited TiBx thin films. Journal of Vacuum Science and Technology A: Vacuum, Surfaces and Films, 2017, 35, .	0.9	40
49	Low-temperature growth of dense and hard Ti0.41Al0.51Ta0.08N films via hybrid HIPIMS/DC magnetron co-sputtering with synchronized metal-ion irradiation. Journal of Applied Physics, 2017, 121, .	1.1	28
50	Control of the metal/gas ion ratio incident at the substrate plane during high-power impulse magnetron sputtering of transition metals in Ar. Thin Solid Films, 2017, 642, 36-40.	0.8	24
51	Gas rarefaction effects during high power pulsed magnetron sputtering of groups IVb and VIb transition metals in Ar. Journal of Vacuum Science and Technology A: Vacuum, Surfaces and Films, 2017, 35, .	0.9	27
52	Phonon and electron contributions to the thermal conductivity of <mml:math xmlns:mml="http://www.w3.org/1998/Math/MathML"><mml:mrow><mml:mi mathvariant="normal">V<mml:msub><mml:mi mathvariant="normal">V<mml:mi>x</mml:mi></mml:mi </mml:msub></mml:mi </mml:mrow></mml:math 	0.9	34
53	epitaxial layers. Physical Review Materials, 2017, 1, . Large-scale molecular dynamics simulations of TiN/TiN(001) epitaxial film growth. Journal of Vacuum Science and Technology A: Vacuum, Surfaces and Films, 2016, 34, .	0.9	30
54	Nitrogen-doped bcc-Cr films: Combining ceramic hardness with metallic toughness and conductivity. Scripta Materialia, 2016, 122, 40-44.	2.6	41

#	Article	IF	CITATIONS
55	Growth, nanostructure, and optical properties of epitaxial VN _x /MgO(001) (0.80 â‰ष्र â‰ष.00) layers deposited by reactive magnetron sputtering. Journal of Materials Chemistry C, 2016, 4, 7924-7938.	2.7	30
56	Interpretation of X-ray photoelectron spectra of carbon-nitride thin films: New insights from in situ XPS. Carbon, 2016, 108, 242-252.	5.4	158
57	Ab Initio Molecular Dynamics Simulations of Nitrogen/VN(001) Surface Reactions: Vacancy-Catalyzed N ₂ Dissociative Chemisorption, N Adatom Migration, and N ₂ Desorption. Journal of Physical Chemistry C, 2016, 120, 12503-12516.	1.5	39
58	Effects of phase stability, lattice ordering, and electron density on plastic deformation in cubic TiWN pseudobinary transition-metal nitride alloys. Acta Materialia, 2016, 103, 823-835.	3.8	56
59	N and Ti adatom dynamics on stoichiometric polar TiN(111) surfaces. Surface Science, 2016, 649, 72-79.	0.8	32
60	Reflection thermal diffuse x-ray scattering for quantitative determination of phonon dispersion relations. Physical Review B, 2015, 92, .	1.1	5
61	Dynamic and structural stability of cubic vanadium nitride. Physical Review B, 2015, 91, .	1.1	71
62	The dynamics of TiNx (x = 1–3) admolecule interlayer and intralayer transport on TiN/TiN(001) islands. Thin Solid Films, 2015, 589, 133-144.	0.8	12
63	Novel hard, tough HfAlSiN multilayers, defined by alternating Si bond structure, deposited using modulated high-flux, low-energy ion irradiation of the growing film. Journal of Vacuum Science and Technology A: Vacuum, Surfaces and Films, 2015, 33, .	0.9	7
64	Strategy for tuning the average charge state of metal ions incident at the growing film during HIPIMS deposition. Vacuum, 2015, 116, 36-41.	1.6	34
65	Al capping layers for nondestructive x-ray photoelectron spectroscopy analyses of transition-metal nitride thin films. Journal of Vacuum Science and Technology A: Vacuum, Surfaces and Films, 2015, 33, .	0.9	33
66	Control of Ti1â^'xSixN nanostructure via tunable metal-ion momentum transfer during HIPIMS/DCMS co-deposition. Surface and Coatings Technology, 2015, 280, 174-184.	2.2	53
67	Self-organized anisotropic (Zr1â~'Si)N nanocomposites grown by reactive sputter deposition. Acta Materialia, 2015, 82, 179-189.	3.8	27
68	Vacancy-induced toughening in hard single-crystal V 0.5 Mo 0.5 N x /MgO(0 0 1) thin films. Acta Materialia, 2014, 77, 394-400.	3.8	75
69	Structure evolution and properties of TiAlCN/VCN coatings deposited by reactive HIPIMS. Surface and Coatings Technology, 2014, 257, 38-47.	2.2	26
70	Novel strategy for low-temperature, high-rate growth of dense, hard, and stress-free refractory ceramic thin films. Journal of Vacuum Science and Technology A: Vacuum, Surfaces and Films, 2014, 32,	0.9	45
71	Effect of WN content on toughness enhancement in V1â^'xWxN/MgO(001) thin films. Journal of Vacuum Science and Technology A: Vacuum, Surfaces and Films, 2014, 32, .	0.9	45
72	Ti adatom diffusion on TiN(001): Ab initio and classical molecular dynamics simulations. Surface Science, 2014, 627, 34-41.	0.8	40

#	Article	IF	CITATIONS
73	Strain-free, single-phase metastable Ti0.38Al0.62N alloys with high hardness: metal-ion energy vs. momentum effects during film growth by hybrid high-power pulsed/dc magnetron cosputtering. Thin Solid Films, 2014, 556, 87-98.	0.8	69
74	X-ray Photoelectron Spectroscopy Analyses of the Electronic Structure of Polycrystalline Ti1-xAlxN Thin Films with 0 â‰â€‰x â‰â€‰0.96. Surface Science Spectra, 2014, 21, 35-49.	0.3	20
75	Elastic constants, Poisson ratios, and the elastic anisotropy of VN(001), (011), and (111) epitaxial layers grown by reactive magnetron sputter deposition. Journal of Applied Physics, 2014, 115, 214908.	1.1	49
76	Ab initio and classical molecular dynamics simulations of N2 desorption from TiN(001) surfaces. Surface Science, 2014, 624, 25-31.	0.8	52
77	Electrochemically tunable thermal conductivity of lithium cobalt oxide. Nature Communications, 2014, 5, 4035.	5.8	137
78	Si incorporation in Ti1â^'xSixN films grown on TiN(001) and (001)-faceted TiN(111) columns. Surface and Coatings Technology, 2014, 257, 121-128.	2.2	25
79	Ti and N adatom descent pathways to the terrace from atop two-dimensional TiN/TiN(001) islands. Thin Solid Films, 2014, 558, 37-46.	0.8	29
80	Physical properties of epitaxial ZrN/MgO(001) layers grown by reactive magnetron sputtering. Journal of Vacuum Science and Technology A: Vacuum, Surfaces and Films, 2013, 31, .	0.9	56
81	Electron/phonon coupling in group-IV transition-metal and rare-earth nitrides. Journal of Applied Physics, 2013, 114, .	1.1	31
82	Sputter-cleaned Epitaxial VxMo(1-x)Ny/MgO(001) Thin Films Analyzed by X-ray Photoelectron Spectroscopy: 3. Polycrystalline V0.49Mo0.51N1.02. Surface Science Spectra, 2013, 20, 80-85.	0.3	8
83	ICMCTF 2013 — Preface. Thin Solid Films, 2013, 549, 1.	0.8	0
84	Improving high-capacity Li1.2Ni0.15Mn0.55Co0.1O2-based lithium-ion cells by modifiying the positive electrode with alumina. Journal of Power Sources, 2013, 233, 346-357.	4.0	139
85	Stretchable batteries with self-similar serpentine interconnects and integrated wireless recharging systems. Nature Communications, 2013, 4, 1543.	5.8	1,169
86	Sputter-cleaned Epitaxial VxMo(1-x)Ny/MgO(001) Thin Films Analyzed by X-ray Photoelectron Spectroscopy: 1. Single-crystal V0.48Mo0.52N0.64. Surface Science Spectra, 2013, 20, 68-73.	0.3	12
87	Toughness enhancement in hard ceramic thin films by alloy design. APL Materials, 2013, 1, .	2.2	109
88	Epitaxial V0.6W0.4N/MgO(001): Evidence for ordering on the cation sublattice. Journal of Vacuum Science and Technology A: Vacuum, Surfaces and Films, 2013, 31, .	0.9	15
89	Sputter-cleaned Epitaxial VxMo(1-x)Ny/MgO(001) Thin Films Analyzed by X-ray Photoelectron Spectroscopy: 2. Single-crystal V0.47Mo0.53N0.92. Surface Science Spectra, 2013, 20, 74-79.	0.3	11
90	Nanolabyrinthine ZrAlN thin films by self-organization of interwoven single-crystal cubic and hexagonal phases. APL Materials, 2013, 1, .	2.2	35

#	Article	IF	CITATIONS
91	Ion-induced surface relaxation: controlled bending and alignment of nanowire arrays. Nanotechnology, 2012, 23, 175302.	1.3	11
92	Microstructure, Oxidation and Tribological Properties of TiAlCN/VCN Coatings Deposited by Reactive HIPIMS. IOP Conference Series: Materials Science and Engineering, 2012, 39, 012011.	0.3	1
93	The Si3N4/TiN Interface: 3. Si3N4/TiN(001) Grown with a â^'150 V Substrate Bias and Analyzed <i>In situ</i> using Angle-resolved X-ray Photoelectron Spectroscopy. Surface Science Spectra, 2012, 19, 52-61.	0.3	2
94	The Si3N4/TiN Interface: 1. TiN(001) Grown and Analyzed <i>In situ</i> using Angle-resolved X-ray Photoelectron Spectroscopy. Surface Science Spectra, 2012, 19, 33-41.	0.3	5
95	The Si3N4/TiN Interface: 5. TiN/Si3N4 Grown and Analyzed <i>In situ</i> using Angle-resolved X-ray Photoelectron Spectroscopy. Surface Science Spectra, 2012, 19, 72-81.	0.3	0
96	Role of ethylene on surface oxidation of TiO2(110). Applied Physics Letters, 2012, 101, 211601.	1.5	2
97	The Si3N4/TiN Interface: An Introduction to a Series of Ultrathin Films Grown and Analyzed <i>In situ</i> using X-ray Photoelectron Spectroscopy. Surface Science Spectra, 2012, 19, 30-32.	0.3	3
98	The Si3N4/TiN Interface: 7. Ti/TiN(001) Grown and Analyzed <i>In situ</i> using X-ray Photoelectron Spectroscopy. Surface Science Spectra, 2012, 19, 92-97.	0.3	1
99	The Si3N4/TiN Interface: 6. Si/TiN(001) Grown and Analyzed <i>In situ</i> using Angle-resolved X-ray Photoelectron Spectroscopy. Surface Science Spectra, 2012, 19, 82-91.	0.3	Ο
100	Dynamics of Ti, N, and TiN <mml:math <br="" xmlns:mml="http://www.w3.org/1998/Math/MathML">display="inline"><mml:msub><mml:mrow></mml:mrow><mml:mi>x</mml:mi></mml:msub></mml:math> (<mml:math) et(<="" td="" tj=""><td>Qq0 0 0 rg 1.1</td><td>gBT /Overlock 47</td></mml:math)>	Qq0 0 0 rg 1.1	gBT /Overlock 47
101	admolecule transport on TiN(001) surfaces. Physical Review B, 2012, 86, . The Si3N4/TiN Interface: 2. Si3N4/TiN(001) Grown with a â°77 V Substrate Bias and Analyzed In situ using Angle-resolved X-ray Photoelectron Spectroscopy. Surface Science Spectra, 2012, 19, 42-51.	0.3	1
102	Configurational disorder effects on adatom mobilities on Ti <mml:math xmlns:mml="http://www.w3.org/1998/Math/MathML" display="inline"><mml:msub><mml:mrow /><mml:mrow><mml:mn>1</mml:mn><mml:mo>a^2 </mml:mo><mml:mi>x</mml:mi>x</mml:mrow>xmlns:mml="http://www.w3.org/1998/Math/MathML" display="inline"><mml:msub><mml:mrow>xmlns:mml="http://www.w3.org/1998/Math/MathML" display="inline"><mml:msub><mml:mrow>xmlns:mml="http://www.w3.org/1998/Math/MathML" display="inline"><mml:msub><mml:msub><mml:mrow>xmlns:mml="http://www.w3.org/1998/Math/MathML" display="inline"><mml:msub><mml:msub><mml:mrow></mml:mrow></mml:msub></mml:msub></mml:mrow></mml:msub></mml:msub></mml:mrow></mml:msub></mml:mrow></mml:msub></mml:mrow </mml:msub><td>> 1.1</td><td>athy3Al<mml:< td=""></mml:<></td></mml:math 	> 1.1	athy3Al <mml:< td=""></mml:<>
103	/> <mml:mi>x</mml:mi> N(001) surfaces from first principles. Physical Review P 2012 85 The Si3N4/TiN Interface: 4. Si3N4/TiN(001) Grown with a â°250 V Substrate Bias and Analyzed <i>In situ</i> using Angle-resolved X-ray Photoelectron Spectroscopy. Surface Science Spectra, 2012, 19, 62-71.	0.3	1
104	Nanodiamond-Based Nanolubricants. Fullerenes Nanotubes and Carbon Nanostructures, 2012, 20, 606-610.	1.0	19
105	Metal versus rare-gas ion irradiation during Ti1â^' <i>x</i> Al <i>x</i> N film growth by hybrid high power pulsed magnetron/dc magnetron co-sputtering using synchronized pulsed substrate bias. Journal of Vacuum Science and Technology A: Vacuum, Surfaces and Films, 2012, 30, .	0.9	98
106	Hierarchically textured Li Mn2â^'O4 thin films as positive electrodes for lithium-ion batteries. Journal of Power Sources, 2012, 206, 288-294.	4.0	10
107	Role of Tin+ and Aln+ ion irradiation (n=1, 2) during Ti1-xAlxN alloy film growth in a hybrid HIPIMS/magnetron mode. Surface and Coatings Technology, 2012, 206, 4202-4211.	2.2	119
108	In situ high-temperature scanning tunneling microscopy study of bilayer graphene growth on 6H-SiC(0001). Thin Solid Films, 2012, 520, 5289-5293.	0.8	3

#	Article	IF	CITATIONS
109	Selection of metal ion irradiation for controlling Ti1â^'xAlxN alloy growth via hybrid HIPIMS/magnetron co-sputtering. Vacuum, 2012, 86, 1036-1040.	1.6	66
110	Long-Range and Local Structure in the Layered Oxide Li _{1.2} Co _{0.4} Mn _{0.4} O ₂ . Chemistry of Materials, 2011, 23, 2039-2050.	3.2	171
111	Enhanced Ge/Si(001) island areal density and self-organization due to P predeposition. Journal of Applied Physics, 2011, 109, 093526.	1.1	2
112	ICMCTF 2011 $\hat{a} \in $ " Preface. Surface and Coatings Technology, 2011, 206, 1511.	2.2	0
113	Real-time control of AlN incorporation in epitaxial Hf1â dl N using high-flux, low-energy (10–40 eV) ion bombardment during reactive magnetron sputter deposition from a Hf0.7Al0.3 alloy target. Acta Materialia, 2011, 59, 421-428.	3.8	20
114	Analytical electron microscopy of Li1.2Co0.4Mn0.4O2 for lithium-ion batteries. Solid State Ionics, 2011, 182, 98-107.	1.3	65
115	Electronic structure of the SiN <mml:math <br="" xmlns:mml="http://www.w3.org/1998/Math/MathML">display="inline"><mml:mrow><mml:msub><mml:mrow /><mml:mrow><mml:mi>x</mml:mi></mml:mrow></mml:mrow </mml:msub></mml:mrow></mml:math> /TiN interface: A model system for superhard nanocomposites. Physical Review B, 2011, 83, .	1.1	42
116	Raman scattering from TiNx (0.67 â‰≇€‰x â‰≇€‰1.00) single crystals grown on MgO(001). Journa Physics, 2011, 110, .	l of Applie	d ₅₄
117	Importance of line and interfacial energies during VLS growth of finely stranded silica nanowires. Journal of Materials Research, 2011, 26, 2247-2253.	1.2	6
118	The Formation and Utility of Sub-Angstrom to Nanometer-Sized Electron Probes in the Aberration-Corrected Transmission Electron Microscope at the University of Illinois. Microscopy and Microanalysis, 2010, 16, 183-193.	0.2	32
119	Electrical characterization of MOS structures with self-organized three-layer gate dielectric containing Si nanocrystals. Journal of Physics: Conference Series, 2010, 253, 012034.	0.3	0
120	ICMCTF 2010. Surface and Coatings Technology, 2010, 205, 1177.	2.2	0
121	Structural Properties of AlN Grown on Sapphire at Plasma Self-Heating Conditions Using Reactive Magnetron Sputter Deposition. Journal of Electronic Materials, 2010, 39, 1146-1151.	1.0	19
122	Effect of oxygen to argon ratio on the properties of thin SiO x films deposited by r.f. sputtering. Journal of Materials Science: Materials in Electronics, 2010, 21, 481-485.	1.1	6
123	Conjugated Carbon Monolayer Membranes: Methods for Synthesis and Integration. Advanced Materials, 2010, 22, 1072-1077.	11.1	50
124	Probing Interfacial Electronic Structures in Atomic Layer LaMnO ₃ and SrTiO ₃ Superlattices. Advanced Materials, 2010, 22, 1156-1160.	11.1	69
125	Local Structure of Layered Oxide Electrode Materials for Lithiumâ€ion Batteries. Advanced Materials, 2010, 22, 1122-1127.	11.1	152
126	Microstructural characterization of thin SiOx films obtained by physical vapor deposition. Materials Science and Engineering B: Solid-State Materials for Advanced Technology, 2010, 174, 132-136.	1.7	21

#	Article	IF	CITATIONS
127	Fully strained low-temperature epitaxy of TiN/MgO(001) layers using high-flux, low-energy ion irradiation during reactive magnetron sputter deposition. Thin Solid Films, 2010, 518, 5169-5172.	0.8	16
128	Formation of Si Nanocrystals in Thin SiO ₂ Films for Memory Device Applications. Materials Science Forum, 2010, 644, 101-104.	0.3	7
129	TiAlCN/VCN nanolayer coatings suitable for machining of Al and Ti alloys deposited by combined high power impulse magnetron sputtering/unbalanced magnetron sputtering. Surface Engineering, 2010, 26, 610-614.	1.1	25
130	Moiré Superstructures of Graphene on Faceted Nickel Islands. ACS Nano, 2010, 4, 6509-6514.	7.3	78
131	Layer-by-Layer Transfer of Multiple, Large Area Sheets of Graphene Grown in Multilayer Stacks on a Single SiC Wafer. ACS Nano, 2010, 4, 5591-5598.	7.3	65
132	Synergistic Compositions of Colloidal Nanodiamond as Lubricant-additive. Journal of Vacuum Science and Technology B:Nanotechnology and Microelectronics, 2010, 28, 869-877.	0.6	37
133	Elastic buckling of AIN ribbons on elastomeric substrate. Applied Physics Letters, 2009, 94, 092104.	1.5	5
134	Highly Sensitive, Mechanically Stable Nanopore Sensors for DNA Analysis. Advanced Materials, 2009, 21, 2771-2776.	11.1	190
135	LEEM investigations of surfaces using a beam of energetic selfâ€ions. Microscopy Research and Technique, 2009, 72, 197-207.	1.2	7
136	Structural study of Li2MnO3 by electron microscopy. Journal of Materials Science, 2009, 44, 5579-5587.	1.7	68
137	Transfer of graphene layers grown on SiC wafers to other substrates and their integration into field effect transistors. Applied Physics Letters, 2009, 95, .	1.5	71
138	Low-temperature vapour–liquid–solid (VLS) growth of vertically aligned silicon oxide nanowires using concurrent ion bombardment. Nanotechnology, 2009, 20, 115607.	1.3	21
139	Growth of Semiconducting Graphene on Palladium. Nano Letters, 2009, 9, 3985-3990.	4.5	307
140	Real-time imaging of surface evolution driven by variable-energy ion irradiation. Ultramicroscopy, 2008, 108, 646-655.	0.8	7
141	Local structure and composition studies of Li1.2Ni0.2Mn0.6O2 by analytical electron microscopy. Journal of Power Sources, 2008, 178, 422-433.	4.0	141
142	Characterization studies of pulse magnetron sputtered hard ceramic titanium diboride coatings alloyed with silicon. Acta Materialia, 2008, 56, 4172-4182.	3.8	17
143	Detection of Single Atoms and Buried Defects in Three Dimensions by Aberration-Corrected Electron Microscope with 0.5-A Information Limit. Microscopy and Microanalysis, 2008, 14, 469-477.	0.2	266
144	Synthesis of linked carbon monolayers: Films, balloons, tubes, and pleated sheets. Proceedings of the National Academy of Sciences of the United States of America, 2008, 105, 7353-7358.	3.3	57

#	Article	IF	CITATIONS
145	Effect of off stoichiometry on Raman scattering from epitaxial and polycrystalline HfNx (0.85≤â‰⊉.50) grown on MgO(001). Journal of Applied Physics, 2008, 104, 033507.	1.1	21
146	Phosphorus incorporation during Si(001):P gas-source molecular beam epitaxy: Effects on growth kinetics and surface morphology. Journal of Applied Physics, 2008, 103, 123530.	1.1	19
147	A Microelectromechanical System for Nano-Scale Testing of One Dimensional Nanostructures. Sensor Letters, 2008, 6, 76-87.	0.4	10
148	Raman scattering from epitaxial TaNx(0.94â‰ജâ‰≇.37) layers grown on MgO(001). Journal of Applied Physics, 2007, 101, 123509.	1.1	35
149	Combined filtered cathodic arc etching pretreatment–magnetron sputter deposition of highly adherent CrN films. Journal of Vacuum Science and Technology A: Vacuum, Surfaces and Films, 2007, 25, 543-550.	0.9	20
150	Interface structure in superhard TiN-SiN nanolaminates and nanocomposites: Film growth experiments andab initiocalculations. Physical Review B, 2007, 75, .	1.1	142
151	Interface microstructure engineering by high power impulse magnetron sputtering for the enhancement of adhesion. Journal of Applied Physics, 2007, 101, 054301.	1.1	247
152	TiN surface dynamics: role of surface and bulk mass transport processes. AIP Conference Proceedings, 2007, , .	0.3	4
153	Growth and physical properties of epitaxial metastable Hf1â^'xAlxN alloys deposited on MgO(001) by ultrahigh vacuum reactive magnetron sputtering. Surface and Coatings Technology, 2007, 202, 809-814.	2.2	21
154	Epitaxial Ti2AlN(0001) thin film deposition by dual-target reactive magnetron sputtering. Acta Materialia, 2007, 55, 4401-4407.	3.8	52
155	Measurement and estimation of temperature rise in TEM sample during ion milling. Ultramicroscopy, 2007, 107, 663-668.	0.8	36
156	Thermally induced self-hardening of nanocrystalline Ti–B–N thin films. Journal of Applied Physics, 2006, 100, 044301.	1.1	50
157	Raman scattering from epitaxial HfN layers grown on MgO(001). Journal of Applied Physics, 2006, 99, 043507.	1.1	17
158	Self-hardening of Nanocrystalline Ti-B-N Thin Films. Microscopy and Microanalysis, 2006, 12, 720-721.	0.2	3
159	Deposition and Properties of Thin (ZrO2)x(Al2O3)1-x Films on Silicon. Plasma Processes and Polymers, 2006, 3, 179-183.	1.6	2
160	Physico-chemical characterization of NF/RO membrane active layers by Rutherford backscattering spectrometryâ~†. Journal of Membrane Science, 2006, 282, 71-81.	4.1	120
161	Two-dimensional island dynamics: Role of step energy anisotropy. Surface Science Reports, 2006, 60, 55-77.	3.8	42
162	Orientation-dependent mobilities from analyses of two-dimensional TiN(111) island decay kinetics. Thin Solid Films, 2006, 510, 339-345.	0.8	7

#	Article	IF	CITATIONS
163	Epitaxial growth of CoSi2 on Si(001) by reactive deposition epitaxy: Island growth and coalescence. Thin Solid Films, 2006, 515, 1340-1348.	0.8	9
164	Influence of ion bombardment on structure and tribological performance of nanoscale multilayer C/Cr PVD coatings. Surface Engineering, 2006, 22, 92-98.	1.1	7
165	Expansion and melting of Xe nanocrystals in Si. Physical Review B, 2006, 74, .	1.1	6
166	Sublimation of Atomic Layers from a Chromium Surface. Physical Review Letters, 2006, 96, 126106.	2.9	16
167	CoSi2 growth on Si(001) by reactive deposition epitaxy: Effects of high-flux, low-energy ion irradiation. Journal of Applied Physics, 2006, 100, 013510.	1.1	4
168	Self-organized lamellar structured tantalum–nitride by UHV unbalanced-magnetron sputtering. Thin Solid Films, 2005, 475, 45-48.	0.8	17
169	Influence of the bias voltage on the structure and the tribological performance of nanoscale multilayer C/Cr PVD coatings. Thin Solid Films, 2005, 475, 219-226.	0.8	66
170	Raman spectroscopy study of C/Cr coatings deposited by the combined steered cathodic ARC/unbalanced magnetron sputtering technique. Surface and Coatings Technology, 2005, 200, 1117-1122.	2.2	14
171	Phase separation and formation of the self-organised layered nanostructure in C/Cr coatings in conditions of high ion irradiation. Surface and Coatings Technology, 2005, 200, 1572-1579.	2.2	42
172	Nucleation kinetics versus nitrogen partial pressure during homoepitaxial growth of stoichiometric TiN(001): A scanning tunneling microscopy study. Surface Science, 2005, 581, L122-127.	0.8	37
173	In situ Transmission Electron Microscopy Studies Enabled by Microelectromechanical System Technology. Journal of Materials Research, 2005, 20, 1802-1807.	1.2	60
174	Self-organized nanocolumnar structure in superhard TiB2 thin films. Applied Physics Letters, 2005, 86, 131909.	1.5	192
175	Nucleation and growth kinetics of spiral steps on TiN(111): Anin situlow-energy electron microscopy study. Journal of Applied Physics, 2005, 98, 034901.	1.1	5
176	Growth of CoSi2 on Si(001) by reactive deposition epitaxy. Journal of Applied Physics, 2005, 97, 044909.	1.1	14
177	Epitaxial and polycrystalline HfNx (0.8⩽x⩽1.5) layers on MgO(001): Film growth and physical properties. Journal of Applied Physics, 2005, 97, 083521.	1.1	95
178	Imaging suspended carbon nanotubes in field-effect transistors configured with microfabricated slits for transmission electron microscopy. Applied Physics Letters, 2005, 87, 173108.	1.5	15
179	Elastic constants of single-crystalTiNx(001)(0.67⩽x⩽1.0)determined as a function ofxby picosecond ultrasonic measurements. Physical Review B, 2005, 71, .	1.1	78
180	Directed Self-Assembly of Ge Nanostructures on Very High Index, Highly Anisotropic Si(hkl) Surfaces. Nano Letters, 2005, 5, 369-372.	4.5	10

#	Article	IF	CITATIONS
181	Growth, surface morphology, and electrical resistivity of fully strained substoichiometric epitaxial TiNx (0.67⩽x<1.0) layers on MgO(001). Journal of Applied Physics, 2004, 95, 356-362.	1.1	118
182	Directed nanostructural evolution in Ti0.8Ce0.2N layers grown as a function of low-energy, high-flux ion irradiation. Applied Physics Letters, 2004, 84, 2796-2798.	1.5	10
183	Growth and physical properties of epitaxial HfN layers on MgO(001). Journal of Applied Physics, 2004, 96, 878-884.	1.1	83
184	Nanomachining carbon nanotubes with ion beams. Applied Physics Letters, 2004, 84, 4484-4486.	1.5	92
185	Dislocation-driven surface dynamics on solids. Nature, 2004, 429, 49-52.	13.7	37
186	Structure and tribological behaviour of nanoscale multilayer C/Cr coatings deposited by the combined steered cathodic arc/unbalanced magnetron sputtering technique. Thin Solid Films, 2004, 447-448, 7-13.	0.8	33
187	Coherent nano-area electron diffraction. Microscopy Research and Technique, 2004, 64, 347-355.	1.2	79
188	Determination of absolute orientation-dependent TiN(001) and TiN(111) step energies. Vacuum, 2004, 74, 345-351.	1.6	7
189	Structure and optical properties of (Al2O3)x(Tio)1â^'x thin films prepared by a sol–gel processing. Vacuum, 2004, 76, 215-218.	1.6	18
190	Magnetic and electric properties of magnetron-sputtered YBCO/LSMO and LSMO/YBCO double layers. Vacuum, 2004, 76, 261-264.	1.6	6
191	Low-energy electron microscopy studies of interlayer mass transport kinetics on TiN(111). Surface Science, 2004, 560, 53-62.	0.8	32
192	Dependence of the electromechanical coupling on the degree of orientation of c-textured thin AlN films. IEEE Transactions on Ultrasonics, Ferroelectrics, and Frequency Control, 2004, 51, 1347-1353.	1.7	55
193	Nucleation kinetics during homoepitaxial growth of TiN(001) by reactive magnetron sputtering. Physical Review B, 2004, 70, .	1.1	45
194	Feature-Scale to Wafer-Scale Modeling and Simulation of Physical Vapor Deposition. The IMA Volumes in Mathematics and Its Applications, 2004, , 219-236.	0.5	0
195	Pathways of atomistic processes on TiN(001) and (111) surfaces during film growth: anab initiostudy. Journal of Applied Physics, 2003, 93, 9086-9094.	1.1	318
196	Microstructural evolution during film growth. Journal of Vacuum Science and Technology A: Vacuum, Surfaces and Films, 2003, 21, S117-S128.	0.9	1,466
197	In-situ nanoindentation of epitaxial TiN/MgO (001) in a transmission electron microscope. Journal of Electronic Materials, 2003, 32, 1023-1027.	1.0	29
198	Determining absolute orientation-dependent step energies: a general theory for the Wulff-construction and for anisotropic two-dimensional island shape fluctuations. Surface Science, 2003, 522, 75-83.	0.8	50

#	Article	IF	CITATIONS
199	In situ high-temperature scanning tunneling microscopy studies of two-dimensional TiN island coarsening kinetics on TiN. Surface Science, 2003, 526, 85-96.	0.8	37
200	Coalescence kinetics of two-dimensional TiN islands on atomically smooth TiN(001) and TiN(111) terraces. Surface Science, 2003, 540, L611-L616.	0.8	17
201	High power pulsed magnetron sputtered CrN films. Surface and Coatings Technology, 2003, 163-164, 267-272.	2.2	242
202	Diagnosis of power fade mechanisms in high-power lithium-ion cells. Journal of Power Sources, 2003, 119-121, 511-516.	4.0	110
203	Experimental evidence for a dissociation mechanism in NH3 detection with MIS field-effect devices. Sensors and Actuators B: Chemical, 2003, 89, 1-8.	4.0	8
204	Structure determination of individual single-wall carbon nanotubes by nanoarea electron diffraction. Applied Physics Letters, 2003, 82, 2703-2705.	1.5	137
205	Structural and mechanical properties of diamond-like carbon films deposited by direct current magnetron sputtering. Journal of Vacuum Science and Technology A: Vacuum, Surfaces and Films, 2003, 21, 851-859.	0.9	20
206	Vacancy hardening in single-crystal TiNx(001) layers. Journal of Applied Physics, 2003, 93, 6025-6028.	1.1	146
207	Growth and physical properties of epitaxial CeN layers on MgO(001). Journal of Applied Physics, 2003, 94, 921-927.	1.1	31
208	Absolute orientation-dependent anisotropic TiN(111) island step energies and stiffnesses from shape fluctuation analyses. Physical Review B, 2003, 67, .	1.1	40
209	Epitaxial Ti1-xWxN alloys grown on MgO(001) by ultrahigh vacuum reactive magnetron sputtering: Electronic properties and long-range cation ordering. Journal of Vacuum Science and Technology A: Vacuum, Surfaces and Films, 2003, 21, 140-146.	0.9	54
210	Microscopy and Spectroscopy of Lithium Nickel Oxide-Based Particles Used in High Power Lithium-Ion Cells. Journal of the Electrochemical Society, 2003, 150, A1450.	1.3	219
211	Nanoparticle beam formation and investigation of gold nanostructured films. Journal of Vacuum Science & Technology an Official Journal of the American Vacuum Society B, Microelectronics Processing and Phenomena, 2003, 21, 2313.	1.6	9
212	Quantitative structure determination of individual carbon nanotubes using nano-area electron diffraction. Microscopy and Microanalysis, 2003, 9, 322-323.	0.2	0
213	Absolute TiN(111) Step Energies from Analysis of Anisotropic Island Shape Fluctuations. Physical Review Letters, 2002, 88, 146101.	2.9	36
214	Size-Dependent Detachment-Limited Decay Kinetics of Two-Dimensional TiN Islands on TiN(111). Physical Review Letters, 2002, 89, 176102.	2.9	32
215	Epitaxial growth of metastable δ-TaN layers on MgO(001) using low-energy, high-flux ion irradiation during ultrahigh vacuum reactive magnetron sputtering. Journal of Vacuum Science and Technology A: Vacuum, Surfaces and Films, 2002, 20, 2007.	0.9	40
216	Growth of single-crystal CrN on MgO(001): Effects of low-energy ion-irradiation on surface morphological evolution and physical properties. Journal of Applied Physics, 2002, 91, 3589-3597.	1.1	117

#	Article	IF	CITATIONS
217	Band gap in epitaxial NaCl-structure CrN(001) layers. Journal of Applied Physics, 2002, 91, 5882-5886.	1.1	117
218	Continuum model of thin film deposition incorporating finite atomic length scales. Journal of Applied Physics, 2002, 92, 3487-3494.	1.1	7
219	Nanophase films deposited from a high-rate, nanoparticle beam. Journal of Vacuum Science & Technology an Official Journal of the American Vacuum Society B, Microelectronics Processing and Phenomena, 2002, 20, 995.	1.6	21
220	Development of preferred orientation in polycrystalline NaCl-structure δ-TaN layers grown by reactive magnetron sputtering: Role of low-energy ion surface interactions. Journal of Applied Physics, 2002, 92, 5084-5093.	1.1	87
221	Electromigration in epitaxial Cu(001) lines. AIP Conference Proceedings, 2002, , .	0.3	7
222	Progress towards Quantitative Electron Nanodiffraction. Microscopy and Microanalysis, 2002, 8, 658-659.	0.2	0
223	Surface changes on LiNi0.8Co0.2O2 particles during testing of high-power lithium-ion cells. Electrochemistry Communications, 2002, 4, 620-625.	2.3	295
224	Phase composition and microstructure of polycrystalline and epitaxial TaNx layers grown on oxidized Si(001) and MgO(001) by reactive magnetron sputter deposition. Thin Solid Films, 2002, 402, 172-182.	0.8	109
225	Optical properties of nanophase films measured by variable-angle spectroscopic ellipsometry. Thin Solid Films, 2002, 408, 211-217.	0.8	9
226	Absolute orientation-dependent TiN() step energies from two-dimensional equilibrium island shape and coarsening measurements on epitaxial TiN() layers. Surface Science, 2002, 513, 468-474.	0.8	44
227	YBCO/LSMO and LSMO/YBCO double-layer deposition by off-axis magnetron sputtering and strain effects. Vacuum, 2002, 69, 243-247.	1.6	8
228	Multiscale Modeling of Thin-Film Deposition: Applications to Si Device Processing. MRS Bulletin, 2001, 26, 182-189.	1.7	74
229	Electronic structure of ScN determined using optical spectroscopy, photoemission, andab initiocalculations. Physical Review B, 2001, 63, .	1.1	139
230	Epitaxial NaCl structure δ-TaNx(001): Electronic transport properties, elastic modulus, and hardness versus N/Ta ratio. Journal of Applied Physics, 2001, 90, 2879-2885.	1.1	88
231	Interfacial reaction pathways and kinetics during annealing of epitaxial Al/TiN(001) model diffusion barrier systems. Thin Solid Films, 2001, 391, 69-80.	0.8	19
232	TiN(001) and TiN(111) island coarsening kinetics: in-situ scanning tunneling microscopy studies. Thin Solid Films, 2001, 392, 164-168.	0.8	48
233	Thermal stability of carbon nitride thin films. Journal of Materials Research, 2001, 16, 3188-3201.	1.2	49
234	Evolution of nanoscale texture in ultrathin TiN films. Applied Physics Letters, 2001, 78, 2223-2225.	1.5	16

#	Article	IF	CITATIONS
235	Interfacial reactions in epitaxial Al/TiN(111) model diffusion barriers: Formation of an impervious self-limited wurtzite-structure AIN(0001) blocking layer. Journal of Applied Physics, 2001, 89, 7841-7845.	1.1	22
236	Optimization ofin situsubstrate surface treatment in a cathodic arc plasma: A study by TEM and plasma diagnostics. Journal of Vacuum Science and Technology A: Vacuum, Surfaces and Films, 2001, 19, 1415-1420.	0.9	31
237	Synchrotron x-ray diffraction and transmission electron microscopy studies of interfacial reaction paths and kinetics during annealing of fully-002-textured Al/TiN bilayers. Journal of Vacuum Science and Technology A: Vacuum, Surfaces and Films, 2001, 19, 182-191.	0.9	17
238	Influence of the interface composition on the corrosion behavior of unbalanced magnetron grown niobium coatings on steel. Journal of Vacuum Science and Technology A: Vacuum, Surfaces and Films, 2001, 19, 1392-1398.	0.9	18
239	Interfacial reaction pathways and kinetics during annealing of 111-textured Al/TiN bilayers: A synchrotron x-ray diffraction and transmission electron microscopy study. Journal of Vacuum Science and Technology A: Vacuum, Surfaces and Films, 2001, 19, 2207-2216.	0.9	12
240	Epitaxial Sc1â^'xTixN(001): Optical and electronic transport properties. Journal of Applied Physics, 2001, 89, 401-409.	1.1	84
241	Quantitative C lattice site distributions in epitaxial Ge1â^'yCy/Ge(001) layers. Journal of Applied Physics, 2001, 90, 3910-3918.	1.1	13
242	Electromigration in Epitaxial Copper Lines. Materials Research Society Symposia Proceedings, 2000, 648, 1.	0.1	4
243	Shortlisted substrate ion etching in combined steered cathodic arc–ubm deposition system: effects on interface architecture, adhesion, and tool performance. Surface Engineering, 2000, 16, 176-180.	1.1	20
244	Channeling-induced asymmetric distortion of depth profiles from polycrystalline-TiN/Ti/TiN(001) trilayers during secondary ion mass spectrometry. Journal of Vacuum Science & Technology an Official Journal of the American Vacuum Society B, Microelectronics Processing and Phenomena, 2000, 18, 1369.	1.6	3
245	Epitaxial CrN(001) Grown and Analyzed In situ by XPS and UPS. II. Analysis of Ar+ Sputter Etched Layers. Surface Science Spectra, 2000, 7, 262-270.	0.3	5
246	Epitaxial VN(001) Grown and Analyzed In situ by XPS and UPS. I. Analysis of As-deposited Layers. Surface Science Spectra, 2000, 7, 221-232.	0.3	9
247	Epitaxial VN(001) Grown and Analyzed In situ by XPS and UPS. II. Analysis of Ar+ Sputter Etched Layers. Surface Science Spectra, 2000, 7, 233-241.	0.3	5
248	Epitaxial ScN(001) Grown and Analyzed In situ by XPS and UPS. II. Analysis of Ar+ Sputter Etched Layers. Surface Science Spectra, 2000, 7, 178-184.	0.3	9
249	Epitaxial ScN(001) Grown and Analyzed In situ by AES After (1) Deposition and (2) Ar+ Sputter Etching. Surface Science Spectra, 2000, 7, 185-192.	0.3	1
250	Epitaxial TiN(001) Grown and Analyzed In situ by AES After (1) Deposition and (2) Ar+ Sputter Etching. Surface Science Spectra, 2000, 7, 213-220.	0.3	2
251	Epitaxial metastable Ge1â~'yCy (y⩼20.02) alloys grown on Ge(001) from hyperthermal beams: C incorporation and lattice sites. Journal of Applied Physics, 2000, 88, 96-104.	1.1	8
252	A Comparison of Auger Electron Spectra from Stoichiometric Epitaxial TiN(001) After (1) UHV Cleaving and (2) Ar+ Sputter Etching. Surface Science Spectra, 2000, 7, 93-100.	0.3	6

#	Article	IF	CITATIONS
253	Epitaxial CrN(001) Grown and Analyzed In situ by XPS and UPS. I. Analysis of As-deposited Layers. Surface Science Spectra, 2000, 7, 250-261.	0.3	10
254	Epitaxial TiN(001) Grown and Analyzed In situ by XPS and UPS. II. Analysis of Ar+ Sputter Etched Layers. Surface Science Spectra, 2000, 7, 204-212.	0.3	21
255	Epitaxial VN(001) Grown and Analyzed In situ by AES After (1) Deposition and (2) Ar+ Sputter Etching. Surface Science Spectra, 2000, 7, 242-249.	0.3	1
256	Epitaxial CrN(001) Grown and Analyzed In situ by AES After (1) Deposition and (2) Ar+ Sputter Etching. Surface Science Spectra, 2000, 7, 271-278.	0.3	0
257	IN-SITU HIGH-TEMPERATURE SCANNING-TUNNELING-MICROSCOPY STUDIES OF TWO-DIMENSIONAL ISLAND-DECAY KINETICS ON ATOMICALLY SMOOTH TIN(001). Surface Review and Letters, 2000, 07, 589-593.	0.5	22
258	Effects of high-flux low-energy ion bombardment on the low-temperature growth morphology of TiN(001) epitaxial layers. Physical Review B, 2000, 61, 16137-16143.	1.1	39
259	In situ X-ray Photoelectron, Ultraviolet Photoelectron, and Auger Electron Spectroscopy Spectra from First-Row Transition-Metal Nitrides: ScN, TiN, VN, and CrN. Surface Science Spectra, 2000, 7, 167-168.	0.3	21
260	Ionized sputter deposition using an extremely high plasma density pulsed magnetron discharge. Journal of Vacuum Science and Technology A: Vacuum, Surfaces and Films, 2000, 18, 1533-1537.	0.9	235
261	Role of fast sputtered particles during sputter deposition: Growth of epitaxialGe0.99C0.01/Ge(001). Physical Review B, 2000, 62, 11203-11208.	1.1	9
262	Texture of Al thin films deposited by magnetron sputtering onto epitaxial W(001). Journal of Applied Physics, 2000, 87, 168-171.	1.1	2
263	Enhanced adhesion through local epitaxy of transition-metal nitride coatings on ferritic steel promoted by metal ion etching in a combined cathodic arc/unbalanced magnetron deposition system. Journal of Vacuum Science and Technology A: Vacuum, Surfaces and Films, 2000, 18, 1718-1723.	0.9	45
264	Epitaxial ScN(001) Grown and Analyzed In situ by XPS and UPS. I. Analysis of As-deposited Layers. Surface Science Spectra, 2000, 7, 169-177.	0.3	4
265	Epitaxial TiN(001) Grown and Analyzed In situ by XPS and UPS. I. Analysis of As-deposited Layers. Surface Science Spectra, 2000, 7, 193-203.	0.3	29
266	Dense fully 111-textured TiN diffusion barriers: Enhanced lifetime through microstructure control during layer growth. Journal of Applied Physics, 1999, 86, 3633-3641.	1.1	125
267	Growth and physical properties of epitaxial metastable cubic TaN(001). Applied Physics Letters, 1999, 75, 3808-3810.	1.5	65
268	A novel pulsed magnetron sputter technique utilizing very high target power densities. Surface and Coatings Technology, 1999, 122, 290-293.	2.2	910
269	Hydrogen uptake in alumina thin films synthesized from an aluminum plasma stream in an oxygen ambient. Applied Physics Letters, 1999, 74, 200-202.	1.5	73
270	Microstructural evolution and Poisson ratio of epitaxial ScN grown on TiN(001)/MgO(001) by ultrahigh vacuum reactive magnetron sputter deposition. Journal of Applied Physics, 1999, 86, 5524-5529.	1.1	68

#	Article	IF	CITATIONS
271	Experimental Methods and Data Analysis for Fluctuation Microscopy. Materials Research Society Symposia Proceedings, 1999, 589, 155.	0.1	8
272	Ion-Implanted Amorphous Silicon Studied by Variable Coherence TEM. Materials Research Society Symposia Proceedings, 1999, 589, 247.	0.1	3
273	Analysis of the Atomic Scale Defect Chemistry in Oxygen Deficient Materials by STEM. Materials Research Society Symposia Proceedings, 1999, 589, 69.	0.1	1
274	Quantitative compositional depth profiling of Si1â^'xâ^'yGexCy thin films by simultaneous elastic recoil detection and Rutherford backscattering spectrometry. Nuclear Instruments & Methods in Physics Research B, 1998, 136-138, 654-660.	0.6	1
275	Microstructure and electronic properties of the refractory semiconductor ScN grown on MgO(001) by ultra-high-vacuum reactive magnetron sputter deposition. Journal of Vacuum Science and Technology A: Vacuum, Surfaces and Films, 1998, 16, 2411-2417.	0.9	112
276	Morphology and microstructure of tensile-strained SiGe(001) thin epitaxial films. Journal of Applied Physics, 1998, 83, 1096-1102.	1.1	13
277	Growth of poly- and single-crystal ScN on MgO(001): Role of low-energy N2+ irradiation in determining texture, microstructure evolution, and mechanical properties. Journal of Applied Physics, 1998, 84, 6034-6041.	1.1	218
278	Improved Ti ₁ –xAl _x N PVD Coatings for Dry High Speed Cutting Operations. Surface Engineering, 1998, 14, 37-42.	1.1	52
279	Morphology of epitaxial TiN(001) grown by magnetron sputtering. Applied Physics Letters, 1997, 70, 1703-1705.	1.5	78
280	Al/TixW1â^'x metal/diffusion-barrier bilayers: Interfacial reaction pathways and kinetics during annealing. Journal of Applied Physics, 1997, 82, 2312-2322.	1.1	16
281	Aluminide formation in polycrystalline Al/W metal/barrier thin-film bilayers: Reaction paths and kinetics. Journal of Applied Physics, 1997, 82, 201-209.	1.1	3
282	Ion energy distributions in reactive arc evaporation discharges used for deposition of TiN films. Surface and Coatings Technology, 1997, 92, 150-156.	2.2	11
283	Large-scale fabrication of hard superlattice thin films by combined steered arc evaporation and unbalanced magnetron sputtering. Surface and Coatings Technology, 1997, 93, 69-87.	2.2	67
284	Microstructure and oxidation-resistance of Ti1 â^' x â^' y â^'zAlxCryYzN layers grown by combined steered-arc/unbalanced-magnetron-sputter deposition. Surface and Coatings Technology, 1997, 94-95, 226-231.	2.2	189
285	In situ scanning tunneling microscopy studies of the evolution of surface morphology and microstructure in epitaxial TiN(001) grown by ultra-high-vacuum reactive magnetron sputtering. Surface and Coatings Technology, 1997, 94-95, 403-408.	2.2	31
286	Ion-assisted growth of Ti1â^'xAlxN/Ti1â^'yNbyN multilayers by combined cathodic-arc/magnetron-sputter deposition. Thin Solid Films, 1997, 302, 179-192.	0.8	117
287	Combined steered arc-unbalanced magnetron grown niobium coatings for decorative and corrosion resistance applications. Surface and Coatings Technology, 1996, 82, 57-64.	2.2	28
288	Development of 111 texture in Al films grown on SiO2/Si(001) by ultrahighâ€vacuum primaryâ€ion deposition. Journal of Vacuum Science and Technology A: Vacuum, Surfaces and Films, 1996, 14, 346-351.	0.9	26

#	Article	IF	CITATIONS
289	Morphology and microstructure of epitaxial Cu(001) films grown by primary ion deposition on Si and Ge substrates. Journal of Applied Physics, 1996, 80, 6699-6705.	1.1	25
290	Origin of compositional variations in sputterâ€deposited TixW1â^'x diffusion barrier layers. Applied Physics Letters, 1995, 67, 3102-3104.	1.5	33
291	Reaction paths and kinetics of aluminide formation in Al/epitaxialâ€W(001) model diffusion barrier systems. Journal of Applied Physics, 1995, 78, 194-203.	1.1	6
292	Lowâ€energy (5 <ei<100 beam<br="" ev),="" for="" highâ€brightness,="" ion="" primary="" source="" ultrahigh="" vacuum="">deposition: Applications for Al and Ge. Journal of Vacuum Science and Technology A: Vacuum, Surfaces and Films, 1995, 13, 2836-2842.</ei<100>	0.9	16
293	Highâ€flux lowâ€energy (â‰,20 eV) N+2ion irradiation during TiN deposition by reactive magnetron sputtering: Effects on microstructure and preferred orientation. Journal of Applied Physics, 1995, 78, 5395-5403.	1.1	229
294	Development of preferred orientation in polycrystalline TiN layers grown by ultrahigh vacuum reactive magnetron sputtering. Applied Physics Letters, 1995, 67, 2928-2930.	1.5	366
295	Mass and energy resolved detection of ions and neutral sputtered species incident at the substrate during reactive magnetron sputtering of Ti in mixed Ar+N2 mixtures. Journal of Vacuum Science and Technology A: Vacuum, Surfaces and Films, 1994, 12, 2846-2854.	0.9	178
296	Directed sputter deposition of AlCu: Film microstructure and microchemistry. Journal of Vacuum Science and Technology A: Vacuum, Surfaces and Films, 1994, 12, 3169-3175.	0.9	25
297	Influence of an external axial magnetic field on the plasma characteristics and deposition conditions during direct current planar magnetron sputtering. Journal of Vacuum Science and Technology A: Vacuum, Surfaces and Films, 1994, 12, 314-320.	0.9	58
298	Influence of the Plasma Kinetics on the Si/C Ratio of aâ€5i _{<i>x</i>} C _{1â€<i>x</i>} : H Thin Films Deposited by Reactive Magnetron Sputtering of a Si Target in Ar + CH ₄ Gas Mixtures. Contributions To Plasma Physics, 1994, 34, 39-49.	0.5	0
299	Single-phase polycrystalline Ti1â^'xWxN alloys (0⩽x⩽0.7) grown by UHV reactive magnetron sputtering: microstructure and physical properties. Thin Solid Films, 1994, 253, 445-450.	0.8	24
300	Reactive sputtering in the ABSTM system. Surface and Coatings Technology, 1993, 56, 179-182.	2.2	29
301	Crystal growth and microstructure of polycrystalline Ti1â^'xAlxN alloy films deposited by ultra-high-vacuum dual-target magnetron sputtering. Thin Solid Films, 1993, 235, 62-70.	0.8	193
302	Decomposition of hexafluoroacetylacetonate Cu(I) vinyltrimethylsilane on, and diffusion of Cu into single crystal and polycrystalline titanium nitride. Surface Science, 1993, 295, 219-229.	0.8	22
303	Comparison of magnetron sputter deposition conditions in neon, argon, krypton, and xenon discharges. Journal of Vacuum Science and Technology A: Vacuum, Surfaces and Films, 1993, 11, 2733-2741.	0.9	54
304	Effects of highâ€flux lowâ€energy (20–100 eV) ion irradiation during deposition on the microstructure and preferred orientation of Ti0.5Al0.5N alloys grown by ultraâ€highâ€vacuum reactive magnetron sputtering. Journal of Applied Physics, 1993, 73, 8580-8589.	1.1	159
305	Average energy deposited per atom: A universal parameter for describing ionâ€assisted film growth?. Applied Physics Letters, 1993, 63, 36-38.	1.5	206
306	Design and characterization of a compact twoâ€ŧarget ultrahigh vacuum magnetron sputter deposition system: Application to the growth of epitaxial Ti1â^'xAlxN alloys and TiN/Ti1â"xAlxN superlattices. Journal of Vacuum Science and Technology A: Vacuum, Surfaces and Films, 1993, 11, 136-142.	0.9	36

#	Article	IF	CITATIONS
307	Interfacial reactions in epitaxial Al/Ti1â^'xAlxN (0≤â‰0.2) model diffusionâ€barrier structures. Journal of Vacuum Science and Technology A: Vacuum, Surfaces and Films, 1993, 11, 11-17.	0.9	41
308	Formation of Defects During Ion-Assisted Growth of Thin Films from the Vapor Phase. Materials Research Society Symposia Proceedings, 1992, 268, 71.	0.1	5
309	Use of an externally applied axial magnetic field to control ion/neutral flux ratios incident at the substrate during magnetron sputter deposition. Journal of Vacuum Science and Technology A: Vacuum, Surfaces and Films, 1992, 10, 3283-3287.	0.9	179
310	Synthesis of metastable epitaxial zincâ€blendeâ€structure AlN by solidâ€state reaction. Applied Physics Letters, 1992, 60, 2491-2493.	1.5	187
311	Polycrystalline TiN films deposited by reactive bias magnetron sputtering: Effects of ion bombardment on resputtering rates, film composition, and microstructure. Journal of Vacuum Science and Technology A: Vacuum, Surfaces and Films, 1992, 10, 265-272.	0.9	208
312	Interfacial reactions in single-crystal-TiN (100)/Al/polycrystalline-TiN multilayer thin films. Thin Solid Films, 1992, 215, 152-161.	0.8	52
313	Growth and microstructure of epitaxial 45°-rotated bcc W layers on NaCl-structure MgO(001) substrates and TiN(001) buffer layers. Journal of Crystal Growth, 1992, 123, 344-356.	0.7	7
314	Lowâ€energy (â^¼100 eV) ion irradiation during growth of TiN deposited by reactive magnetron sputtering: Effects of ion flux on film microstructure. Journal of Vacuum Science and Technology A: Vacuum, Surfaces and Films, 1991, 9, 434-438.	0.9	157
315	Defect structure and phase transitions in epitaxial metastable cubic Ti0.5Al0.5N alloys grown on MgO(001) by ultraâ€highâ€vacuum magnetron sputter deposition. Journal of Applied Physics, 1991, 69, 6437-6450.	1.1	141
316	Transmission electron microscopy studies of microstructural evolution, defect structure, and phase transitions in polycrystalline and epitaxial Ti1â^'xAlxN and TiN films grown by reactive magnetron sputter deposition. Thin Solid Films, 1991, 205, 153-164.	0.8	80
317	Effects of an unbalanced magnetron in a unique dual-cathode, high rate reactive sputtering system. Thin Solid Films, 1990, 193-194, 117-126.	0.8	45
318	COmparison of Some Basic Plasma Parameters and Discharge Characteristics of Planar Magnetron Sputtering Discharges in Argon and Neon. Contributions To Plasma Physics, 1990, 30, 223-231.	0.5	21
319	Deposition of carbon films by bias magnetron sputtering in neon and argon. Thin Solid Films, 1990, 185, 247-256.	0.8	12
320	Growth of TaC thin films by reactive direct current magnetron sputtering: Composition and structure. Journal of Vacuum Science and Technology A: Vacuum, Surfaces and Films, 1990, 8, 3769-3778.	0.9	21
321	The dc magnetron sputter deposition process of YBa 2 Cu 3 O x thin films. Physica C: Superconductivity and Its Applications, 1989, 162-164, 599-600.	0.6	0
322	Effect of ion bombardment during growth on the electrical resistivity of magnetron-sputtered carbon films. Thin Solid Films, 1989, 168, 239-248.	0.8	13
323	Microstructure modification of TiN by ion bombardment during reactive sputter deposition. Thin Solid Films, 1989, 169, 299-314.	0.8	308
324	Electrostatic Probe Measurements in the Glow Discharge Plasma of a D. C. Magnetron Sputtering System. Contributions To Plasma Physics, 1988, 28, 157-167.	0.5	62

#	Article	IF	CITATIONS
325	Influence of the Basic Process Parameters on the Ion/Atom Arrival Rate Ratio during Magnetron Sputter Deposition of Thin Carbon Films. Contributions To Plasma Physics, 1988, 28, 265-273.	0.5	9
326	Highly oriented ZnO films obtained by d.c. reactive sputtering of a zinc target. Thin Solid Films, 1984, 120, 55-67.	0.8	57
327	Atomic concentrations of binary compound thin films on elemental substrates determined by Rutherford backscattering techniques. Journal of Applied Physics, 1983, 54, 1358-1364.	1.1	16
328	Angular distribution and sputtering yield of Al and Al2O3 during 40 key argon ion bombardment. Vacuum, 1982, 32, 747-752.	1.6	7
329	The mechanism of d.c. reactive sputtering. Thin Solid Films, 1981, 85, 300.	0.8	0
330	Direct current reactive sputtering of aluminium. Thin Solid Films, 1978, 52, 365-371.	0.8	16
331	Study of High Surface Area Alumina and Ga-Alumina Materials for Denox Catalyst Applications. Ceramic Engineering and Science Proceedings, 0, , 499-504.	0.1	Ο